Exact Solutions of Electro-Osmotic Flow of Generalized Second-Grade Fluid with Fractional Derivative in a Straight Pipe of Circular Cross Section

Shaowei Wang[a,b], Moli Zhao[a,b], Xicheng Li[c], Xi Chen[d], and Yanhui Ge[e]

[a] Department of Engineering Mechanics, School of Civil Engineering, Shandong University, Jinan 250061, P.R. China
[b] Geotechnical and structural engineering research center, Shandong University, Jinan 250061, P.R. China
[c] School of Mathematical Sciences, University of Jinan, 106 Jiwei Road, 250022, Jinan, P.R. China
[d] Department of Mechanics and Engineering Science, State Key Laboratory for Turbulence and Complex Systems, College of Engineering, Peking University, Beijing 100871, P.R. China
[e] College of Civil Engineering, Shandong Jiaotong University, Jinan 250357, P.R. China

Reprint requests to S. W.; E-mail: shaoweiwang@sdu.edu.cn

Z. Naturforsch. **69a**, 697 – 704 (2014) / DOI: 10.5560/ZNA.2014-0066
Received May 28, 2014 / revised August 28, 2014 / published online November 20, 2014

The transient electro-osmotic flow of generalized second-grade fluid with fractional derivative in a narrow capillary tube is examined. With the help of the integral transform method, analytical expressions are derived for the electric potential and transient velocity profile by solving the linearized Poisson–Boltzmann equation and the Navier–Stokes equation. It was shown that the distribution and establishment of the velocity consists of two parts, the steady part and the unsteady one. The effects of retardation time, fractional derivative parameter, and the Debye–Hückel parameter on the generation of flow are shown graphically.

Key words: Analytical Solutions; Fractional Calculus; Laplace Transform; Viscoelastic Fluids; Electro-Osmotic Flow.

1. Introduction

With the development of microfluidic devices and their applications in microelectromechanical systems and microbiological sensors [1, 2], the research field of electro-osmosis (EO) has become very attractive. Recently, some researchers [3, 4] pointed out that the micelle structure of polymer electrolyte membranes (PEMs) might consist of only cylindrical nanochannels, which facilitate water and proton transport, rather than large water pore clusters connected by smaller nano-channels as in Gierke's model. This raises the problem that how to model the fluids electro-osmotic flow in a straight pipe of circular cross section.

Most of the theoretical researches on electro-osmotic flow are limited to the fully developed steady-state flow [5 – 8]. An electro-osmotic flow problem in an infinite cylindrical pore with a uniform surface charge density has been studied analytically by Berg and Ladipo [9]. The results reveal the distribution of the electric potential and the counter-ions (protons), the velocity profile of the water flow and its associated total flux, as well as the protonic current, conductivity, and water drag. Chang [10] presented a theoretical study on the transient electro-osmotic flow through a cylindrical microcapillary containing a salt-free medium for both constant surface charge density and constant surface potential. The exact solutions for the electric potential distribution and the transient electro-osmotic flow velocity are derived by solving the nonlinear Poisson–Boltzmann equation and the Navier–Stokes equation. With the application of a stepwise voltage, Mishchuk and González-Caballero studied a theoretical model of electro-osmotic flow in a wide capillary [11]. Both periodical and aperiodical flow regimes were studied with arbitrary pulse/pulse or pulse/pause durations and amplitudes.

On the other hand, microfluidic devices are usually used to analyze biofluids, which are often solutions of long chain molecules and their behaviour is very different from that of Newtonian fluids, such as memory effects, normal stress effect, yield stress, etc. These fluids can not be treated as Newtonian fluids. Many researchers have recently focused on non-Newtonian fluid behaviour of biofluids in electrokinetically driven microflows. The first research of non-Newtonian effects to electro-osmotic flow was done by Das and Chakraborty [12, 13]. In their studies, the biofluids were treated as power-law fluids, and the analytical solution, describing the transport characteristics of a non-Newtonian fluid flow in a rectangular microchannel, was obtained under the sole influence of electrokinetic effects. For the same non-Newtonian fluid model, Zhao and Yang [14] obtained the general Smoluchowski velocity for electro-osmosis over a surface with arbitrary zeta potentials. Park and Lee [15] derived a semi-analytical expression for the Helmholtz–Smoluchowski velocity under pure electro-osmosis conditions for the full Phan-Thien–Tanner (PTT) constitutive equation, and they used a finite volume method to calculate numerically the flow of the full PTT model in a rectangular duct under the action of electro-osmosis and a pressure gradient [16]. By using the PTT constitutive model, Choi et al. [17] studied the electro-osmotic flow of viscoelastic fluids analytically. Assuming a planar interface between two viscoelastic immiscible fluids, Afonso et al. considered a steady two-fluid electro-osmotic stratified flow in a planar microchannel [18]. Bandopadhyay et al. [19] derived the flow patterns for a linearized Maxwell fluid in presence of modulated surface charges on microchannel walls in presence of a time-periodic electric field. Through the combined deployment of viscoelastic fluids and oscillatory driving pressure forces, Bandopadhyay and Chakraborty [20] reported a mechanism of massive augmentations in energy harvesting capabilities of nanofluidic devices.

As one kind of typical biofluid, it is well known that blood is constituted of a suspension of many asymmetric, relatively large viscoelastic particles: it is a inhomogeneous, anisotropic, polarized, composite fluid. While it has long been well established that blood is essentially a 'shear-thinning fluid', i.e., apparent viscosity decreases with increase in shear rate, the validity of existing constitutive models for different flow geometries over microscopic length scales remains yet to be rigorously tested and justified [13]. Massoudi and Phuoc [21] used a modified second-grade fluid model to study the pulsatile flow of blood in an artery, and they pointed out that the modified second-grade fluid is the simplest constitutive model that can describe shear-thinning (or shear-thickening) and normal stress differences. In recent years, fractional calculus has encountered much success in the description of viscoelastic non-Newtonian fluids flow. The constitutive equations with fractional derivative have been found to be quite flexible in describing the viscoelastic behaviour of non-Newtonian fluids. In past decades, many researchers studied the unsteady flow of generalized second-grade fluids [22 – 25].

In the present study, the non-Newtonian behaviour of biofluids is modelled by the generalized second-grade fluid with fractional derivative. Although for some viscoelastic fluids, such as polymeric liquids, there is a depletion layer in the vicinity of the wall, which leads to the formation of a Newtonian layer close to the wall and therefore alters the flow physics, we do not consider the effect of depletion layer in the present study. So it is important to mention here that we consider the case of no depletion layer formation such that there is only one region in the channel. The purpose of this paper is to present the analytical solution of unsteady electro-osmotic flow of generalized second-grade fluid in a cylindrical capillary, and to discuss the effects of physical parameters, such as the retardation time, fractional derivative parameter, and the Debye–Hückel parameter on the generation of flow.

2. Governing Equations

2.1. Constitutive Equation of Generalized Second-Grade Fluid

The continuity equation for an incompressible fluid is

$$\nabla \cdot \mathbf{V} = 0\,. \tag{1}$$

In one dimension, the constitutive equation of generalized second-grade fluid can be expressed in terms of [26]

$$\tau = \mu\gamma + \mu\lambda_{\mathrm{r}}^{\alpha}\frac{\mathrm{d}^{\alpha}}{\mathrm{d}t^{\alpha}}\gamma, \tag{2}$$

where τ is the shear stress, γ is the shear strain, μ is viscosity constant, λ_{r} is the retardation time of viscoelastic fluids, α is the fractional parameter such that

$0 \le \alpha \le 1$, and $\mathrm{d}^\alpha / \mathrm{d}t^\alpha$ is the Caputo fractional derivative [27]

$$\frac{\mathrm{d}^\alpha}{\mathrm{d}t^\alpha} f(t) = \frac{1}{\Gamma(\alpha-1)} \int_0^t \frac{f'(\tau)}{(t-\tau)^\alpha} \mathrm{d}\tau . \tag{3}$$

2.2. Mathematical Model of the Flow

Consider the electro-osmotic flow of generalized second-grade fluid of dielectric constant ε, at rest at time $t \le 0$, contained in a straight pipe of circular cross section and radius R. It is assumed that the pipe wall is uniformly charged with a zeta potential, ψ_w. When an external electric field E_0 is imposed along the axial direction, the fluid in the pipe sets in motion due to electro-osmosis, as shown in Figure 1.

All quantities are referred to cylindrical polar coordinates (r, θ, z), where r is measured from the axis of the pipe and z along it. If we assume a velocity distribution of the form

$$(0, 0, u(r,t)), \ \ 0 \le r \le R, \ \ t > 0, \tag{4}$$

the initial condition is given by

$$u(r,0) = 0, \ \ 0 \le r \le R, \tag{5}$$

and the equation of continuity (1) is satisfied automatically.

According to the theory of electrostatics, the net charge density ρ_e is expressed by a potential distribution ψ, which is given by the Poison equation,

$$\begin{aligned} \nabla^2 \psi &= \frac{1}{r}\frac{\partial}{\partial r}\left(r \frac{\partial \psi}{\partial r}\right) + \frac{1}{r^2}\frac{\partial^2 \psi}{\partial \theta^2} + \frac{\partial^2 \psi}{\partial z^2} \\ &= -\frac{\rho_\mathrm{e}}{\varepsilon}, \end{aligned} \tag{6}$$

where ε is the dielectric constant of the solution in the pipe. The boundary condition is that the zeta potential ψ_w is given on the wall of the pipe,

$$\psi(R, \theta) = \psi_\mathrm{w}, \ \ \left.\frac{\partial \psi}{\partial r}\right|_{r=0} = 0. \tag{7}$$

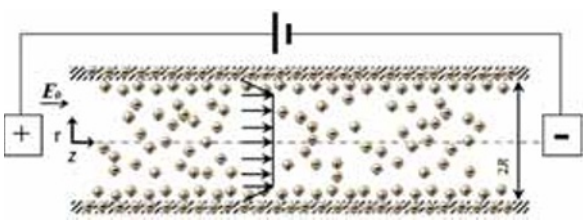

Fig. 1. Schematic of the electro-osmotic flow in a microchannel (from [28]).

For pure electro-osmotic flows (i.e., absent of any pressure gradients) of incompressible liquids, the Navier–Stokes equations take the following form [29, 30],

$$\rho \frac{\partial \mathbf{v}}{\partial t} = \mu \nabla^2 \mathbf{v} + \rho_\mathrm{e} \mathbf{E}(\omega t), \tag{8}$$

where $\mathbf{v}$ is the flow velocity, t is the time, ρ is the fluid density, μ is the fluid viscosity, and $E(\omega t)$ is a general time-periodic function with a frequency ω, which describes the applied electric field strength. In present research, we assume that the charge distribution in the Debye layer is not affected by time, i.e., it has a constant electric potential E_0, then the relevant equation of motion reduces to

$$\rho \frac{\partial u}{\partial t} = \frac{1}{r}\frac{\partial}{\partial r}(r \tau_{rz}) + \rho_\mathrm{e} E_0, \tag{9}$$

which has the following initial and boundary conditions:

$$u(r,0) = \left.\frac{\partial u}{\partial r}\right|_{r=0} = 0, \tag{10}$$

$$u(r,t) = 0, \ \ r = R. \tag{11}$$

3. Exact Solution for the Model

Neglecting all non-electrostatic interactions between the ions including the ionic finite size, i.e., here we assume that the ions are point sized, for small values of electrical potential ψ of the electrical double layer (EDL), the Debye–Hückel approximation can be used successfully, which means physically that the electrical potential is small compared with the thermal energy of the charged species. So we have the linearized charge density

$$\rho_\mathrm{e} = -\frac{2 z_v^2 e^2 n_0 \psi}{k_\mathrm{B} T}, \tag{12}$$

where z_v is the valence of ions, e is the fundamental charge, k_B is the Boltzmann constant, and T is the absolute temperature.

With the help of the Debye–Hückel approximation [31, 32], (6) can be linearized to

$$\frac{1}{r}\frac{\partial}{\partial r}\left(r \frac{\partial \psi}{\partial r}\right) = \kappa^2 \psi. \tag{13}$$

Then the equation of motion (9) becomes

$$\rho \frac{\partial u}{\partial t} = \frac{1}{r}\frac{\partial}{\partial r}(r \tau_{rz}) - \kappa^2 \varepsilon \psi E_0 \tag{14}$$

Here $\kappa = \left(\frac{2z_{\mathrm{v}}^2 e^2 n_0}{\varepsilon k_{\mathrm{B}} T}\right)^{1/2}$ is the Debye–Hückel parameter and κ^{-1} characterizes the thickness of the EDL.

In cylindrical coordinates, (2), i.e., the constitutive equation for generalized second-grade fluid with fractional derivative, can be expressed as

$$\tau_{rz} = \mu \frac{\partial u}{\partial r} + \mu \lambda_{\mathrm{r}}^{\alpha} \frac{\partial^{\alpha}}{\partial t^{\alpha}} \left(\frac{\partial u}{\partial r}\right). \tag{15}$$

Eliminating τ_{rz} from (14) and (15) yields

$$\rho \frac{\partial u}{\partial t} + \kappa^2 \varepsilon \psi E_0 = \mu \left(1 + \lambda_{\mathrm{r}}^{\alpha} \frac{\partial^{\alpha}}{\partial t^{\alpha}}\right) \cdot \left[\frac{1}{r}\frac{\partial}{\partial r}\left(r \frac{\partial u}{\partial r}\right)\right]. \tag{16}$$

Introducing the below listed non-dimensional parameters,

$$\psi^* = \frac{\psi}{\psi_{\mathrm{w}}}, \quad u^* = \frac{u}{u_s}, \quad r^* = \frac{r}{R}, \quad t^* = \frac{\mu}{R^2 \rho} t, \quad u_s = -\frac{\varepsilon \psi_{\mathrm{w}} E_0}{\mu}, \tag{17}$$

and substituting the above normalized variables into (13), (16) and the initial boundary conditions (7), (10), (11) yields (for simplicity, the non-dimensional symbol "*" is omitted hereafter)

$$\frac{1}{r}\frac{\partial}{\partial r}\left(r \frac{\partial \psi}{\partial r}\right) = K^2 \psi, \tag{18}$$

$$\frac{\partial u}{\partial t} - K^2 \psi = \left(1 + \lambda \frac{\partial^{\alpha}}{\partial t^{\alpha}}\right) \cdot \left[\frac{1}{r}\frac{\partial}{\partial r}\left(r \frac{\partial u}{\partial r}\right)\right], \tag{19}$$

$$\psi(1) = 1, \quad \left.\frac{\partial \psi}{\partial r}\right|_{r=0} = 0, \tag{20}$$

$$u(r,0) = \left.\frac{\partial u}{\partial r}\right|_{r=0} = 0, \tag{21}$$

$$u(r,t) = 0, \quad r = 1, \tag{22}$$

where $K = \kappa R$ is called the non-dimensional electrokinetic width, and $\lambda = \left(\frac{\lambda_{\mathrm{r}} \mu}{R^2 \rho}\right)^{\alpha}$ is the normalized retardation time.

The solution of problem (18) and (20) is

$$\psi(r) = \frac{I_0(Kr)}{I_0(K)}, \tag{23}$$

where I_0 is the zero-order modified Bessel function of the first kind. In order to get the exact solution of the model, we introduce the Laplace transform and inverse Laplace transform,

$$\bar{u}(r,s) = \int_0^{\infty} u(r,t)\, \mathrm{e}^{-st}\, \mathrm{d}t, \tag{24}$$

$$u(r,t) = \frac{1}{2\pi i} \int_{\sigma - i\infty}^{\sigma + i\infty} \bar{u}(r,s)\, \mathrm{e}^{st}\, \mathrm{d}s, \tag{25}$$

and the Hankel transform and its inverse,

$$\tilde{u}(\beta_m, t) = \int_0^1 r u(r,t) J_0(\beta_m r)\, \mathrm{d}r, \tag{26}$$

$$u(r,t) = 2 \sum_{m=1}^{\infty} \frac{J_0(\beta_m r)}{J_1^2(\beta_m)} \tilde{u}(\beta_m, t), \tag{27}$$

where J_0 is the zero-order Bessel function of the first kind, the β_m values are the positive roots of $J_0(\beta) = 0$. Substituting $\psi(r)$ into (19), then using Laplace transform and Hankel transform with respect to t and r, respectively, results in the solution of velocity in the Hankel–Laplace domain

$$\tilde{\bar{u}}(\beta_m, s) = \frac{K^2 \tilde{\psi}(\beta_m)}{s[s + (1 + \lambda s^{\alpha})\beta_m^2]}. \tag{28}$$

Here we use the Laplace transform formula for the Caputo fractional derivative [27]

$$\mathcal{L}\left\{\frac{\mathrm{d}^p}{\mathrm{d}t^p} f(t)\right\} = s^p F(s) - \sum_{k=0}^{n-1} s^{p-k-1} f^{(k)}(0), \quad n - 1 < p < n, \tag{29}$$

where $F(s) = \mathcal{L}\{f(t)\}$.

Applying the Hankel transform to (18) yields the expression for $\tilde{\psi}(\beta_m)$ as

$$\tilde{\psi}(\beta_m) = \frac{\beta_m J_1(\beta_m)}{\beta_m^2 + K^2}, \tag{30}$$

using the operational property of finite Hankel transform for derivatives,

$$\int_0^1 r \left[f''(r) + \frac{1}{r} f'(r)\right] J_0(\beta_m r)\, \mathrm{d}r = -\beta_m^2 \tilde{f}(\beta_m) + \beta_m f(1) J_1(\beta_m). \tag{31}$$

Substituting (30) into (28) and using inverse Hankel and Laplace transforms, we can obtain the analytical

solution

$$u(r,t) = 1 - \frac{I_0(Kr)}{I_0(K)} - 2K^2 \sum_{m=1}^{\infty} \frac{U(\beta_m,t) J_0(\beta_m r)}{\beta_m(\beta_m^2 + K^2) J_1(\beta_m)}, \tag{32}$$

where

$$U(\beta_m,t) = \sum_{n=0}^{\infty} \frac{(-1)^n \beta_m^{2n-1}}{n!} t^n E^{(n)}_{1-\alpha,n\alpha+1}(-\lambda\beta_m^2 t^{1-\alpha}) + \sum_{n=0}^{\infty} \frac{(-1)^n \lambda \beta_m^{2n}}{n!} t^{n+1-\alpha} E^{(n)}_{1-\alpha,(n+1)\alpha+2}(-\lambda\beta_m^2 t^{1-\alpha}), \tag{33}$$

and $E^{(n)}_{\alpha,\beta}$ is the nth derivative of the Mittag–Leffler function [27], which is defined by the following series:

$$E_{\alpha,\beta}(z) = \sum_{k=0}^{\infty} \frac{z^k}{\Gamma(\alpha k + \beta)}. \tag{34}$$

4. Spacial Cases

4.1. Steady Flow for $t \to \infty$

When $t \to \infty$, $U(\beta_m,t) \to 0$ and the flow in the tube becomes a steady flow, and (32) becomes

$$u(r,t) = 1 - \frac{I_0(Kr)}{I_0(K)}, \tag{35}$$

which is the distribution of a steady velocity profile in the capillary.

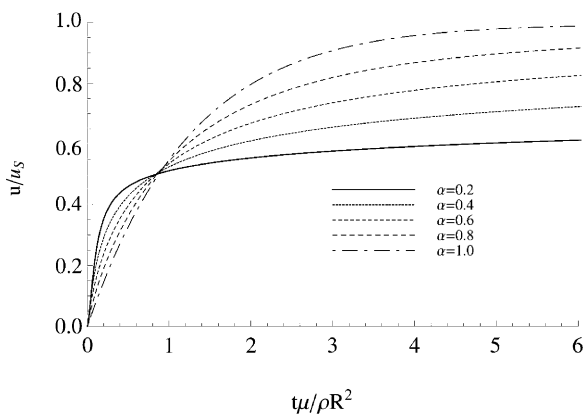

Fig. 2. Dimensionless velocity profiles of generalized second-grade fluid with fractional derivative for different α at the centre of the pipe.

4.2. Newtonian Fluid Model

The Newtonian fluid is a special kind of generalized second-grade fluid with $\lambda = 0$. From general formula (28), the exact solution can be expressed as

$$u(r,t) = 2K^2 \sum_{m=0}^{\infty} \left[1 - e^{-\beta_m^2 t}\right] \frac{J_0(\beta_m r)}{\beta_m^2 J_1^2(\beta_m)} \bar{\psi}(\beta_m), \tag{36}$$

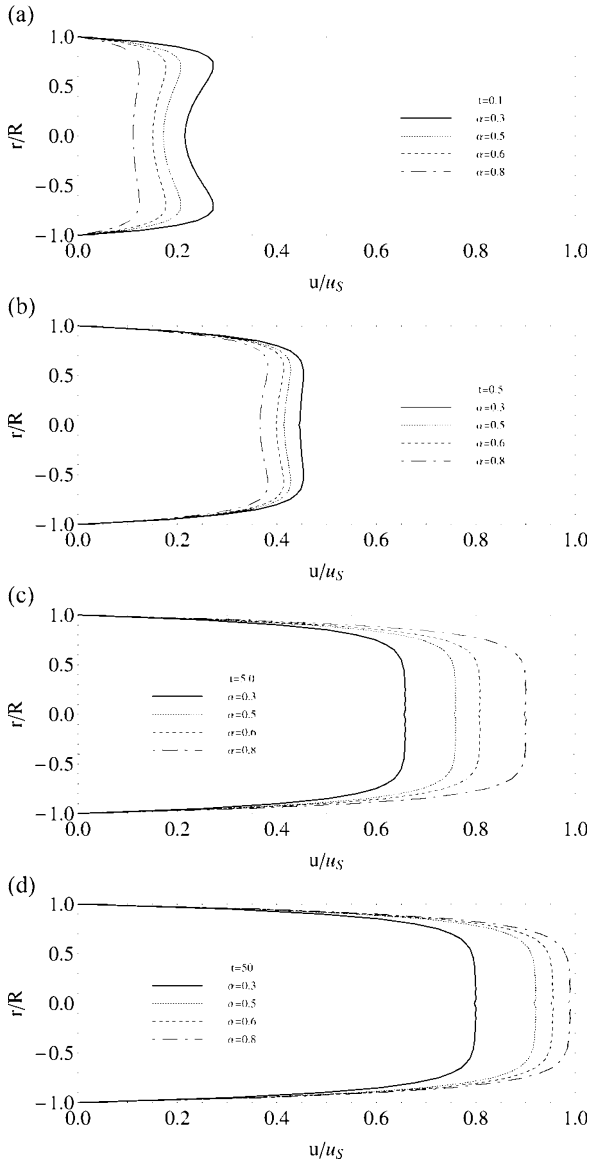

Fig. 3. Electroosmotic flow velocity distributions for different fractional derivative parameter α. (a) $t = 0.1$; (b) $t = 0.5$; (c) $t = 5$; (d) $t = 50$.

or another from:

$$u(r,t) = 1 - \frac{I_0(Kr)}{I_0(K)} - 2K^2 \sum_{m=0}^{\infty} \frac{e^{-\beta_m^2 t} J_0(\beta_m r)}{\beta_m(\beta_m^2 + K^2) J_1(\beta_m)}. \tag{37}$$

Equation (36) has the same form with the result obtained by Kang et al. [33] using the Green's function method. Obviously, the advantage of the solution in this paper, (37), is its simplicity, which is resolved into two parts. The steady part

$$1 - \frac{I_0(Kr)}{I_0(K)} \tag{38}$$

is known and consistent with the result given by Rice and Whitehead [34], and the rest is the unsteady one.

4.3. Standard Second-Grade Fluid Model

When $\lambda \neq 0$ and $\alpha = 1$ in (32), we get the solution for a second-grade fluid, which takes the form

$$u(r,t) = 1 - \frac{I_0(Kr)}{I_0(K)} - 2K^2 \sum_{m=0}^{\infty} \exp\left\{-\frac{\beta_m^2 t}{1+\lambda\beta_m^2}\right\} \frac{J_0(\beta_m r)}{\beta_m(\beta_m^2 + K^2) J_1(\beta_m)}. \tag{39}$$

Furthermore, the above expression reduces to the result for a Newtonian fluid, i.e., (36) when $\lambda = 0$.

5. Results and Discussion

As is known to all, the fractional parameter α plays an important and fundamental role of constructing different fractional models. We now first study the start-up pipe flow for the fractional second-grade model. Figure 2 shows the generation of flow for different values of α at the centre of the pipe. Without loss of generality, these curves were constructed with $\lambda = 1$ and $K = 10$. It is of interest to investigate that the fractional derivative parameter α greatly affects the velocity profiles. In a short time, the flow for the generalized second-grade fluid model with smaller fractional derivative parameter is easier to start up. It is because of the smaller α means that the elasticity of the viscoelastic fluid is in a dominant position, the driving force deriving from the applied external electric field is more effective to be transmitted in the viscoelastic fluid, so the generalized second-grade fluid with smaller α is easier to be driven by the applied electric field. Although the decreasing fractional derivative parameter α accelerates the flow of the fluid in a short time, the smaller α makes the elastic behaviour of the fluid be dominant, which helps the fluid to be at rest. Whatever to say, the corresponding generalized second-grade fluid model always represents a fluid-like property. As time t progresses enough, the center velocity finally tends to the steady state flow, indicated by $1 - I_0(10r)/I_0(10) \approx 1.0$, and it is reached much faster for a smaller value of fractional parameter α. The same phenomenon of the effect of fractional derivative parameter on the velocity profiles can be found in Figures 3 and 4, which present the velocity profiles for increasing specific values of α and increasing times, respectively.

When $\alpha = 0.6$, the effect of K on the generation of flow at the centre of the pipe is shown graphically in Figure 3. As shown in the figure, the decreasing K dampen the velocity amplitude. Particularly, the steady velocity tends to 1.0 when $K \gg 1$. In fact, asymptotic expansions show that $I_0(Kr)/I_0(K)$ can be negligible when $K \gg 1$.

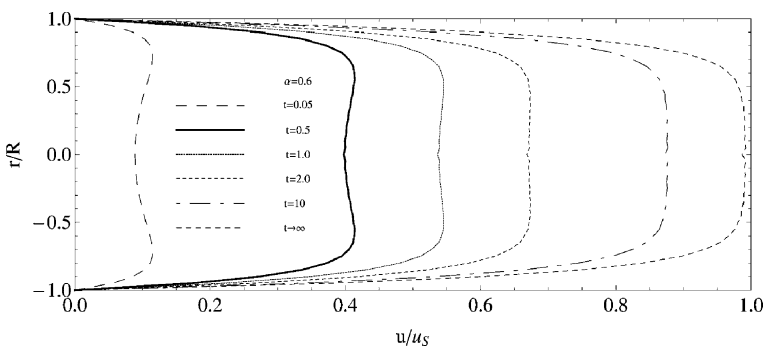

Fig. 4. Generation of steady electroosmotic flow velocity when $\alpha = 0.6$.

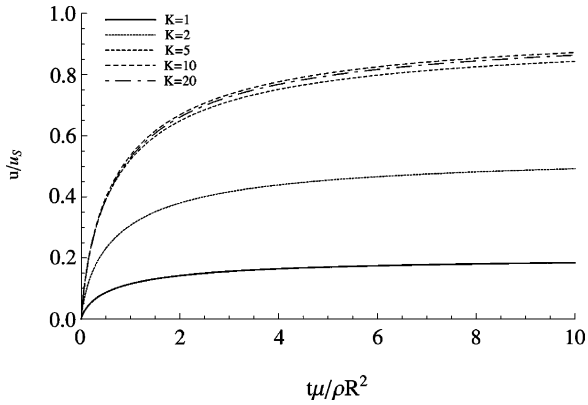

Fig. 5. Effect of K on the generation of velocity at the centre of pipe.

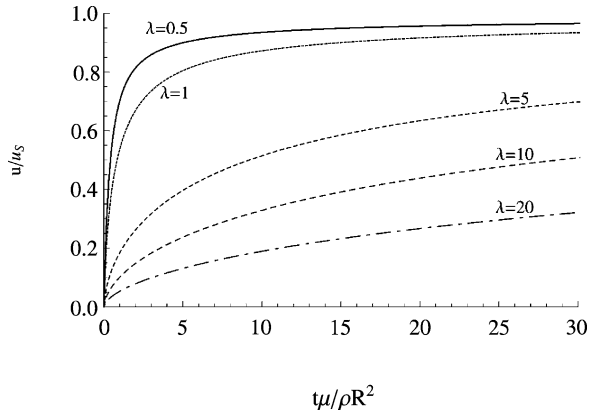

Fig. 6. Effect of λ on the distribution of velocity at the centre of pipe.

Figure 4 gives the curves of the center velocity with respect to t for various values of λ when $\alpha = 0.6$ and $K = 10$. It can be observed that the increasing retardation time stabilizes the flow in the tube. When λ is very small, $\lambda \to 0$, the fractional second-grade model (2) reduces to the classical Newtonian fluid model, and the behaviour of the flow will tend to that of a Newtonian fluid. In addition, for greater values of retardation time, it needs more time to reach the steady state flow. Physically, larger retardation time of any viscoelastic fluid enhances the viscoelastic effect of the fluid, and makes it to need more time for the stress respond to deformation, which results in a decrease in its unsteady flow velocity.

6. Conclusion

An analytical solution of the unsteady electro-osmotic flow of a fractional second-grade fluid in a capillary under the Debye–Hückel approximation is presented in this work. The solution involves solving the linearized Poisson–Boltzmann equation, together with the Cauchy momentum equation and the constitutive equation of viscoelastic fluids considering the electro-osmotic forces as the body forces. With the method of integral transform, the distributions of velocity profiles in the capillary are obtained analytically. The effects of retardation time, fractional derivative parameter, and the Debye–Hückel parameter on the generation of flow have been analyzed numerically. The normalized steady state velocity increases monotonically to 1 with the increasing Debye–Hückel parameter.

Appendix

The Derivation of (32) and (33)

Substituting (30) into (28) yields the solution in the dual-transform domain

$$\tilde{\bar{u}}(\beta_m, s) = K^2 \cdot \frac{\beta_m J_1(\beta_m)}{\beta_m^2 + K^2} \cdot \frac{1}{s[s + (1+\lambda s^\alpha)\beta_m^2]}. \quad \text{(A1)}$$

Applying partial fractions and Taylor series yields

$$\begin{aligned} &\frac{1}{s\,[s + (1+\lambda s^\alpha)\beta_m^2]} \\ &= \frac{1}{s\beta_m^2} - \frac{1}{\beta_m^2} \cdot \frac{1+\lambda\beta_m^2 s^{\alpha-1}}{s + (1+\lambda s^\alpha)\beta_m^2} \\ &= \frac{1}{s\beta_m^2} - \sum_{n=0}^{\infty} (-1)^n \frac{\beta_m^{2(n-1)} s^{-(n+1)\alpha}}{(s^{1-\alpha} + \lambda\beta_m^2)^{n+1}} \\ &- \sum_{n=0}^{\infty} (-1)^n \frac{\lambda\beta_m^{2n} s^{-n\alpha-1}}{(s^{1-\alpha} + \lambda\beta_m^2)^{n+1}}. \end{aligned} \quad \text{(A2)}$$

Then by using the formula of Laplace transform of the Mittag–Leffler function [27]

$$\mathcal{L}^{-1}\left\{\frac{k!\,s^{\alpha-\beta}}{(s^\alpha \mp a)^{k+1}}\right\} = t^{\alpha k+\beta-1} E_{\alpha,\beta}^{(k)}(\pm a t^\alpha), \quad \text{(A3)}$$

we can get (33).

Acknowledgement

This work is supported by the National Natural Science Foundation of China (Nos.11002083, 51279093, 41302225), the National Basic Research Program

of China (2013CB0360000), the Shandong Province Young and Middle-aged Research Awards Fund (No. BS2012SW002) and the Doctor Foundations of the University of Jinan (No. XBS1209).

[1] H. A. Stone, A. D. Stroock, and A. Ajdari, Annu. Rev. Fluid Mech. **36**, 381 (2004).
[2] T. Bayraktar and S. B. Pidugu, Int. J. Heat Mass Transfer **49**, 815 (2006).
[3] G. Gebel, Polymer **41**, 5829 (2000).
[4] K. Schmidt-Rohr and Q. Chen, Nat. Mater. **7**, 75 (2008).
[5] K. Horiuchi and P. Dutta, Int. J. Heat Mass Transfer **47**, 3085 (2004).
[6] S. Chakraborty, Int. J. Heat Mass Transfer **49**, 810 (2006).
[7] A. Sharma and S. Chakraborty, Int. J. Heat Mass Transfer **51**, 4875 (2008).
[8] A. Sadeghi, M. Saidi, and A. A. Mozafari, Int. J. Heat Mass Transfer **54**, 4069 (2011).
[9] P. Berg and K. Ladipo, Proc. R. Soc. A **465**, 2663 (2009).
[10] S. H. Chang, Biomicrofluidics **3**, 012802 (2009).
[11] N. A. Mishchuk and F. González-Caballero, Electrophoresis **27**, 650 (2006).
[12] S. Das and S. Chakraborty, Anal. Chim. Acta **559**, 15 (2006).
[13] S. Chakraborty, Anal. Chim. Acta **605**, 175 (2007).
[14] C. Zhao and C. Yang, Electrophoresis **31**, 973 (2010).
[15] H. M. Park and W. M. Lee, J. Colloid Interface Sci. **317**, 631 (2008).
[16] H. M. Park and W. M. Lee, Lab-on-Chip **8**, 1163 (2008).
[17] W. Choi, S. W. Joo, and G. Lim, J. Non-Newtonian Fluid Mech. **187 – 188**, 1 (2012).
[18] A. M. Afonso, M. A. Alves, and F. T. Pinho, J. Colloid Interface Sci. **395**, 277 (2013).
[19] A. Bandopadhyay, U. Ghosh, and S. Chakraborty, J. Non-Newtonian Fluid Mech. **202**, 1 (2013).
[20] A. Bandopadhyay and S. Chakraborty, Appl. Phys. Lett. **101**, 043905 (2012).
[21] M. Massoudi and T. X. Phuoc, Comput. Math. Appl. **56**, 199 (2008).
[22] W. Tan and M. Xu, Mech. Res. Commun. **29**, 3 (2002).
[23] M. Athar, M. Kamran, and M. Imran, Meccanica **47**, 603 (2012).
[24] C. Fetecau, C. Fetecau, and M. Rana, Z. Naturforsch. **66a**, 753 (2011).
[25] M. El-Shahed and A. Salem, Z. Naturforsch. **59a**, 829 (2004).
[26] M. Xu and W. Tan, Sci. China Ser. A **44**, 1387 (2001).
[27] I. Podlubny, Fractional Differential Equations, Academic Press, New York 1999.
[28] A. M. Afonso, M. A. Alves, and F. T. Pinho, J. Non-Newtonian Fluid Mech. **159**, 50 (2009).
[29] C. Yang and D. Li, Colloids Surf. A **143**, 339 (1998).
[30] P. Dutta and A. Beskok, Anal. Chem. **73**, 5097 (2001).
[31] J. H. Masliyah and S. Bhattacharjee, Electrokinetic and Colloid Transport Phenomena, Willey Interscience, Hoboken, NJ 2006.
[32] D. Li, Electrokinetics in Microfluidics, Elsevier, Amsterdam 2004.
[33] Y. Kang, C. Yang, and X. Huang, Int. J. Eng. Sci. **40**, 2203 (2002).
[34] C. L. Rice and R. Whitehead, J. Phys. Chem. **69**, 4017 (1965).